

## Cobalt – Copper – Manganese

*Lazar Rokhlin, Evgeniya Lysova, Nataliya Bochvar*

### Introduction

Based on the adjoining binary phase diagrams, [1909Jae] suggested a possible configuration for the Co-Cu-Mn phase diagram. It was characterized by the existence of a three-phase monovariant peritectic transformation region extending from the Cu-Mn side to the  $\gamma(\text{Cu}, \gamma\text{Mn}, \alpha\text{Co})$  ternary solid solution and by the absence of an invariant transformation during crystallization. Such constitution of the Co-Cu-Mn phase diagram was confirmed by the theoretical work of [1942Hir], who used calculations of the free energy of the alloys. The Co-Cu-Mn phase diagram was studied experimentally by [1938Koe] using thermal, magnetic and microstructural analyses in the region from the Co-Cu side up to 40 mass% Mn. A partial liquidus surface and the monovariant line bounding the field of joint crystallization of the  $\gamma(\text{Cu}, \gamma\text{Mn}, \alpha\text{Co})$  and  $(\alpha\text{Co})$  solid solutions were constructed. In addition, the isolines of Curie temperature from 20 to 800°C were drawn assuming them as tie lines between the  $\gamma(\text{Cu}, \gamma\text{Mn}, \alpha\text{Co})$  and  $(\alpha\text{Co})$  solid solutions. [1938Koe] also constructed four vertical sections at 10, 20, 30 and 40 mass% Mn. [1958Top1, 1958Top2] studied Mn rich alloys with up to 50 mass% Co and up to 50 mass% Cu, which had been annealed at 500°C. The studied alloys contained  $(\alpha\text{Mn})$  and  $(\gamma\text{Mn})$  solid solutions. The results of [1958Top1, 1958Top2] contradict, however, the Co-Mn phase diagram through the existence of an extended  $(\beta\text{Mn})$  solid solution [1979Cha]. [1982Has] investigated phase compositions of Co-Cu-Mn alloys at several temperatures in the range 877 to 1277°C. Based on their own experimental data, six isothermal sections of the phase diagram were presented. [1979Dri, 1979Cha] reviewed the Co-Cu-Mn phase diagram using data from [1938Koe] and [1958Top1, 1958Top2].

The methods and composition ranges studied in the different investigations are described in Table 1.

### Binary Systems

The binary Co-Cu and Cu-Mn systems are accepted from the MSIT Evaluation Program after [2006Ans] and [2005Tur], respectively. The Co-Mn phase diagram is taken from [Mas2].

### Solid Phases

No ternary compound has been found in the Co-Cu-Mn system. Three binary ordered phases,  $\gamma_1$ ,  $\gamma_2$  and  $\gamma_3$ , have been established in the Cu-Mn system. There are extended solid solutions based on the separate allotropic forms of the pure metals. Characteristics of the solid phases of the Co-Cu-Mn system are shown in Table 2.

### Liquidus, Solidus and Solvus Surfaces

The partial liquidus surface of the Co-Cu-Mn ternary system is shown in Fig. 1. The region adjoining the Co-Cu side is divided by a monovariant line into a surface corresponding to the primary crystallization of the  $(\alpha\text{Co})$  and  $\gamma$  primary solid solutions. The monovariant line corresponds to the  $L + (\alpha\text{Co}) \rightleftharpoons (\text{Cu})$  peritectic reaction, the temperature of which falls from 1113.3°C at the Co-Cu binary down to ~800°C on the addition of ~45 at.% Mn. Its location is taken from [1938Koe] with a little correction necessary to meet the accepted Co-Cu binary diagram [2006Ans]. Taking into consideration the binary systems Co-Mn and Cu-Mn, the liquidus surface in the Mn rich region should include a surface of primary crystallization of the  $(\beta\text{Mn})$  and  $(\delta\text{Mn})$  solid solutions. The location of these surfaces has not been established.

Figure 2 shows the partial solidus surface in the region adjoining the Co-Cu side. It is divided by a double saturation line (which bounds the  $L + (\alpha\text{Co}) + \gamma$  three-phase region) into the surface of the joint crystallization of  $(\alpha\text{Co}) + \gamma$  and termination of the ternary  $\gamma$  solid solution. The double saturation line bounding the three-phase region is drawn after [1938Koe] with a small correction to meet the binary Co-Cu

[2006Ans]. In accordance with [1938Koe], tie lines corresponding to the isolines of Curie temperature are shown on the concentration field outlined by the double saturation line.

### Isothermal Sections

Isothermal sections at different temperatures are presented in Figs. 3-8. They were taken from the calculations of [1982Has] with some corrections to meet the accepted binary phase diagrams.

### Temperature – Compositions Sections

Two vertical sections are shown in Figs. 9 and 10. They are drawn according to [1938Koe] with some corrections to meet the accepted binary phase diagrams. In accordance with the accepted Cu-Mn phase diagram, the sections must cross the  $\gamma_3$ ,  $(\alpha\text{Mn}) + \gamma_3$  and  $(\alpha\text{Mn}) + \gamma_2$  areas which are shown in the vertical sections only approximately.

### Notes on Materials Properties and Applications

The Co-Cu-Mn system forms part of the commercial alloy SA04 (AP Cu-Mn-28Ni-29Co5-Si-B) used for the soldering of hot and corrosion resistant steels and alloys. The soldering temperature is 1050°C and its seal strength is 350 MPa.

[1947Fre] discovered the propensity for alloys containing 2-4 mass% Co and up to 15 mass% Mn to age harden at temperatures of 480, 540 and 595°C.

[1973Mas] established the anti-ferromagnetic behavior of Mn rich Co-Cu-Mn alloys and their Elinvar characteristics. Nonmagnetic ternary alloys of 32.8 - ~87.5% Mn and less than 67% Cu and 24% Co (mass%) were found to have pronounced Elinvar characteristics and fairly good corrosion resistance.

[1976Ano] reported that Co-Cu-Mn alloys with a typical composition of 10%Co-58%Cu-31.5%Mn (mass%) can be successfully used as brazing materials for gas turbine applications in place of alloys containing expensive precious metals.

[2003Cao] investigated the magnetic properties of the Mn layer-doped Co/Cu<sub>92</sub>Mn<sub>8</sub>/Co layered structures. Their behavior in magnetic fields was established.

A summary of studies of the materials properties and applications related to the Co-Cu-Mn alloys is presented in Table 3.

### References

- [1909Jae] Jänecke, E., “Ternary Alloys of Cu, Ag, Au; Cr, Mn; Fe, Co, Ni; Pd. Pt Metals” (in German), *Z. Phys. Chem.*, **67**, 668-688 (1909) (Experimental, Phase Diagram, Phase Relations, 23)
- [1938Koe] Köster, W., Wagner, E., “The Ternary Co-Mn-Cu System” (in German), *Z. Metallkd.*, **30**, 352-353 (1938) (Experimental, Phase Diagram, Magn. Prop., #, 3)
- [1942Hir] Hirone, T., Katayama, T., “On the Constitution of the Ternary Alloys”, *Sci. Rep. Tohoku Imp. Univ.*, **30**, 109-124 (1942) (Calculation, Phase Diagram, 9)
- [1947Fre] Frederickson, J.W., “Age Hardening Copper - Cobalt - Manganese Alloys”, *Trans. ASM*, **38**, 593-617 (1947) (Experimental, Mechan. Prop., 8)
- [1958Top1] Topchiashvili, L.I., “The Influence of Iron, Cobalt, and Nickel on the Structure and Properties of Mn-Cu Alloys”, *Russ. J. Inorg. Chem. (Engl. Transl.)*, **3**, 253-256 (1958) (Experimental, Mechan. Prop., Electr. Prop., 0)
- [1958Top2] Topchiashvili, L.I., Agladze, R.I., Mokhov, V.M., “Investigation of Mn-Cu-Co Alloys” (in Russian), *Zh. Neorg. Khim.*, **3**(11), 2537-2544 (1958) (Experimental, Mechan. Prop., Electr. Prop., 5)
- [1973Mas] Masumoto, H., Sawaya S., Kikuchi, M., “Nonmagnetic Elinvar – Type Alloys in the Mn-Cu-Co System”, *Trans. JIM*, **14**(1), 56-61, (1973) (Experimental, Mechan. Prop., 5)
- [1976Ano] Anon, “Cu-Mn-Co Braze Alloy Beats Precious Metals”, *Mater. Eng.*, **83**(1), 20 (1976) (Mechan. Prop., 0)

- [1979Cha] Chang, Y.A., Neumann, J.P., Mikula, A., Goldberg, D., "Co-Cu-Mn", *INCRA Monograph Series 6 Phase Diagrams and Thermodynamic Properties of Ternary Copper-Metall Systems*, NSRD, Washington, 422-425 (1979) (Phase Diagram, Phase Relations, Review, 3)
- [1979Dri] Drits, M.E., Bochvar, N.R., Guzei, L.S., Lysova, E.V., Padezhnova, E.M., Rokhlin, L.L., Turkina, N.I., "Cu-Co-Mn" in *"Binary and Multicomponent Copper - Base Systems"* (in Russian), Abrikosov, N.X., (Eds.), Nauka, Moscow, 145-148 (1979) (Phase Diagram, Review, 2)
- [1982Has] Hasebe, M., Oikawa, K., Nishizawa, T., "Computer Calculation of Phase Diagrams of Co-Cu-Mn and Co-Cu-Ni Systems", *Nippon Kinzoku Gakkai Shi*, **46**(6), 584-590 (1982) (Calculation, Phase Diagram, #, 18)
- [2003Cao] Cao, R., Ye, J., Zhao, Y., Jin, Q.Y., Wang, H., "Study of Magnetoresistance in Mn Layer-Doped Co/Cu/Co Multilayers", *Phys. Status Solidi A*, **195**(2), 434-439 (2003) (Experimental, Magn. Prop., 7)
- [2005Tur] Turchanin, M., Agraval, P., Groeber, J., Matusch, D., Turkevich, V., "Cu-Mn (Copper-Manganese)", MSIT Binary Evaluation Program, in *MSIT Workplace*, Effenberg, G. (Ed.), MSI, Materials Science International Services GmbH, Stuttgart; Document ID: 20.14136.1.20, (2005) (Phase Diagram, Phase Relations, Crys. Structure, Thermodyn., Assessment, 25)
- [2006Ans] Ansara I., Ivanchenko, V., Turchanin M., Agraval P., "Co-Cu (Cobalt-Copper)", MSIT Binary Evaluation Program, in *MSIT Workplace*, Effenberg, G. (Ed.), MSI, Materials Science International Services, GmbH, Stuttgart; to be published, (2006) (Phase Diagram, Phase Relations, Crys. Structure, Thermodyn., Assessment, 19)

**Table 1:** Investigations of the Co-Cu-Mn Phase Relations, Structures and Thermodynamics

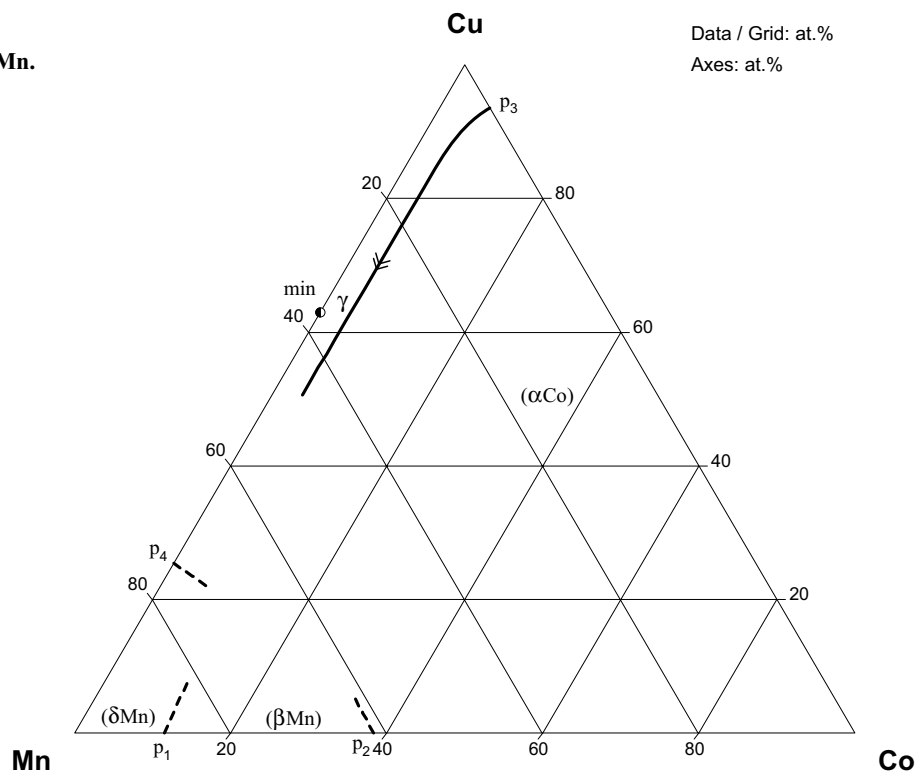
Reference	Method/Experimental Technique	Temperature/Composition/Phase Range Studied
[1938Koe]	Thermal, magnetic, microstructural analyses	Alloys with constant Mn = 10, 20, 30, 40 mass%. Temperature - composition sections at constant Mn = 10, 20, 30, 40 mass%. Liquidus surface with monovariant peritectic line and miscibility gap in solid state.
[1958Top1, 1958Top2]	Melting in a high - frequency furnace in pressed and sintered magnesite crucibles, casting in mild steel mold, homogenization at 900-800-700-600-500°C for 1 day at each temperature and added 500°C for 20 days in sealed quartz ampoules. Metallographic, hardness, resistivity, dilatometry.	Alloys in the Mn corner (100 - 50 mass% Mn) up to 50 mass% Co and 50 mass% Cu. These alloys have a two-phase structure in the annealed state: ( $\alpha$ Mn) and ( $\gamma$ Mn, $\alpha$ Co)
[1982Has]	Ternary diffusion couple technique, computer calculation	Experimental results on the miscibility gap ( $\gamma$ and $\gamma^f$ ) between 877 and 1077°C and on the $\gamma$ /L equilibrium between 1277 and 977°C. Six calculated isothermal sections at 1177, 1077, 977, 877, 777 and 577°C

**Table 2:** Crystallographic Data of Solid Phases

Phase/ Temperature Range [°C]	Pearson Symbol/ Space Group/ Prototype	Lattice Parameters [pm]	Comments/References
$\gamma$ , (Cu, $\gamma$ Mn, $\alpha$ Co) < 1495	<i>cF4</i> <i>Fm<math>\bar{3}m</math></i> Cu		
(Cu) < 1084.62		$a = 361.46$	pure Cu at 25°C [Mas2] dissolves 9.1 at.% Co at 1113.3°C [Mas2] and 100% Mn [2005Tur]
( $\gamma$ Mn) 1138 - 1087		$a = 386.0$	pure $\gamma$ Mn [Mas2] dissolves up to 5 at.% Co at 1138°C [Mas2] and 100 at.% Cu [2005Tur]
( $\alpha$ Co) 1495 - 422		$a = 354.47$ $a = 356.88$	[Mas2] at 520°C [2006Ans] dissolves 11.7 at.% Cu at 1113.3°C and ~59 at.% Mn at 1161°C [Mas2]
( $\epsilon$ Co) < 422	<i>hP2</i> <i>P6<math>_3</math>/mmc</i> Mg	$a = 250.71$ $c = 406.86$	at 25°C [Mas2]
( $\delta$ Mn) 1246 - 1138	<i>cI12</i> <i>Im<math>\bar{3}m</math></i> W	$a = 308.0$	dissolves 9.0 at.% Co at ~1185°C [Mas2] and 13 at.% Cu at 1097°C [2005Tur]
( $\beta$ Mn) 1087 - 707	<i>cP20</i> <i>P4<math>_1</math>32</i> $\beta$ Mn	$a = 631.52$	dissolves 41 at.% Co at 1161°C [Mas2] and 2.03 at.% Cu at 706°C [2005Tur]
( $\alpha$ Mn) < 707	<i>cI58</i> <i>I<math>\bar{4}3m</math></i> $\alpha$ Mn	$a = 891.26$	dissolves up to 3 at.% Co [Mas2] and 2.3 at.% Cu at 706°C [2005Tur]
$\gamma_3$ (Cu-Mn phase) $\leq 700$	<i>c**</i>	-	[2005Tur]
$\gamma_2$ , MnCu <sub>3</sub> $\leq 450$	<i>c**</i>	-	[2005Tur]
$\gamma_1$ , MnCu <sub>5</sub>	<i>c**</i>	-	[2005Tur]

**Table 3:** Investigations of the Co-Cu-Mn Materials Properties

Reference	Method/Experimental Technique	Type of Property
[1947Fre]	Melting in a high - frequency induction furnace, cold - worked and solution - treated for 0.5 h at temperatures varying from 650 to 980°C, aging at temperatures from 315 to 650°C for times of 0.5, 1, 2, 4, 8, 16, 24 and 48 h	Time - hardness curves at various aging temperatures for cold - reduced and annealed Co-Cu-Mn alloys with 2, 3 and 4 mass% Co and 1 and 10 mass% Mn
[1973Mas]	Measurement of Young's modulus at -150 - ~400°C, rigidity modulus and hardness at room temperature. The resonance frequency 470 - 880 Hz. Annealing temperature - 900°C, cold working or water quenching and reheating for 1 h at 200, 400, 600 and 800°C	Elinvar characteristics for Co-Cu-Mn alloys of 0 - ~40.0 mass% Co, 0.1 - ~67.0 mass% Cu, 38.0 - ~88 mass% Mn subjected to various heat treatments and cold working. Nonmagnetic Elinvar - type alloys consisted of less than 67 mass% Cu, 24 mass% Co and 32.8 - ~87.5 mass% Mn and have fairly good corrosion resistance
[1976Ano]	Tensile, shear and fatigue strength	The alloy with 10 mass% Co, 58 mass% Mn and 31.5 mass% Cu can be used as brazing materials in place of alloys of precious metals
[2003Cao]	Magnetic Properties	Giant magnetoresistance in Mn layer - doped Co/Cu/Co multilayers

**Fig. 1: Co-Cu-Mn.**  
Liquidus surface  
projection

**Fig. 2: Co-Cu-Mn.**  
Solidus surface with  
isolines of Curie  
temperature

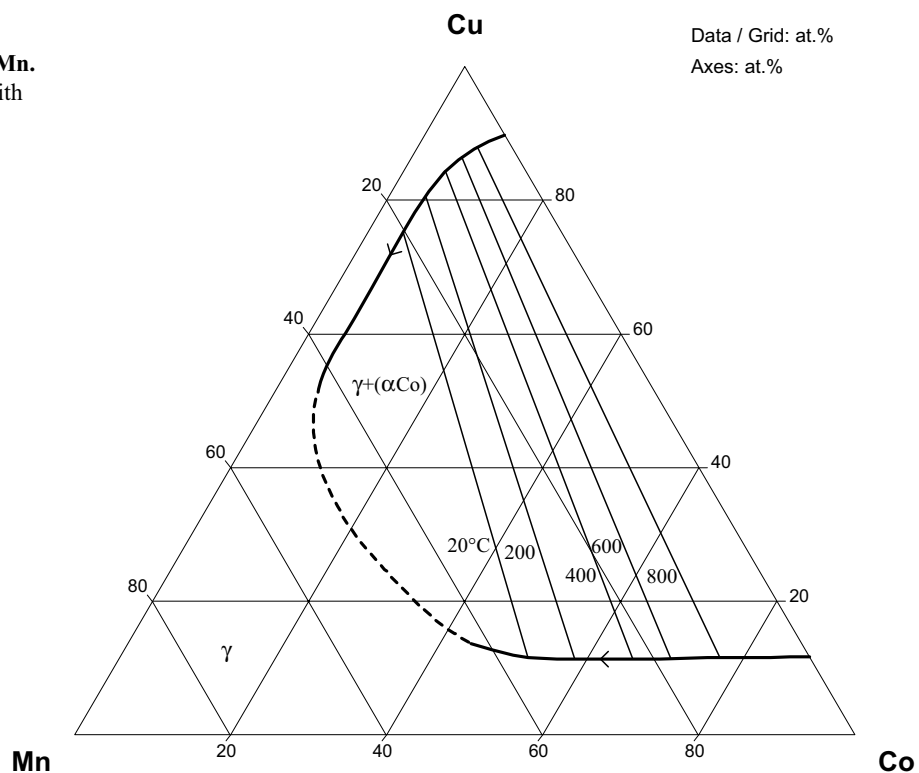


**Fig. 3: Co-Cu-Mn.**  
Isothermal section at  
1777°C

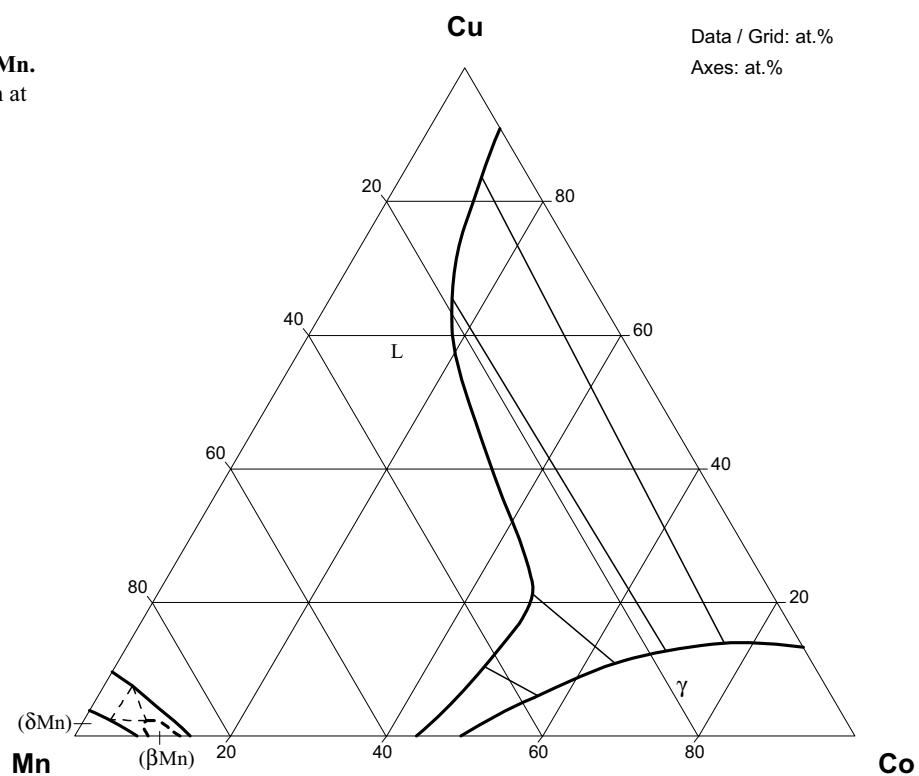


**Fig. 4: Co-Cu-Mn.**  
Isothermal section at  
1077°C

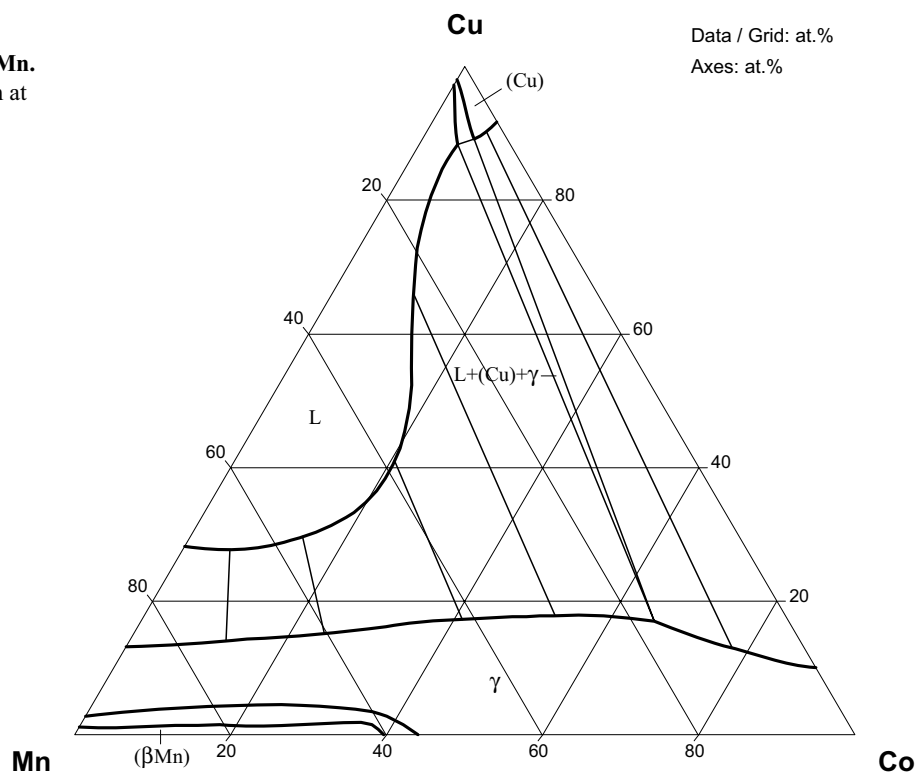


**Fig. 5: Co-Cu-Mn.**  
Isothermal section at  
977°C

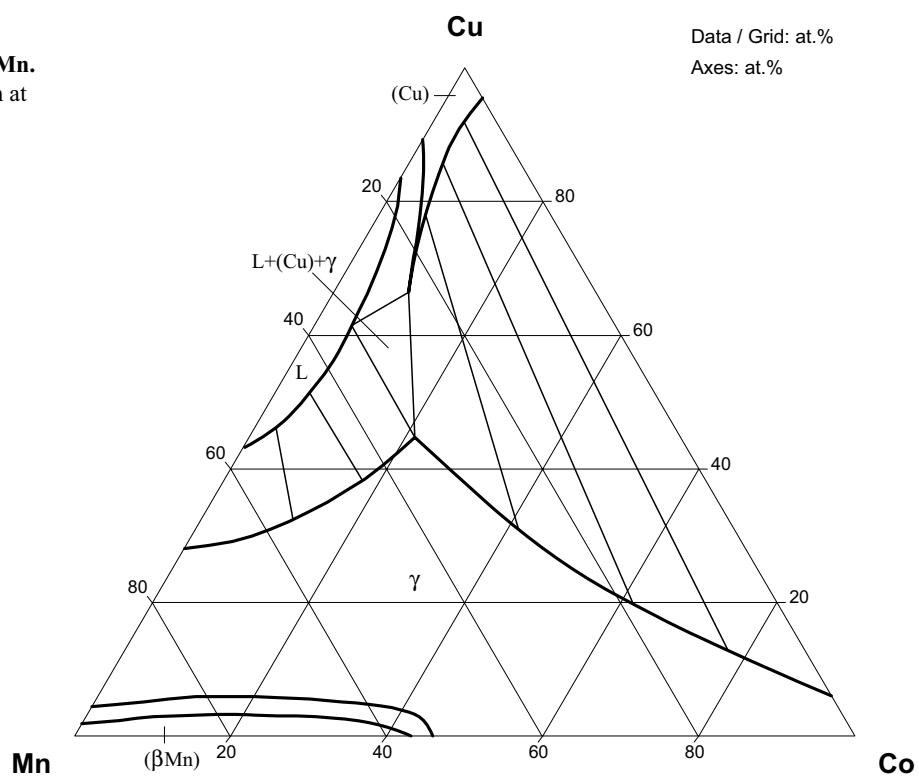


**Fig. 6: Co-Cu-Mn.**  
Isothermal section at  
877°C

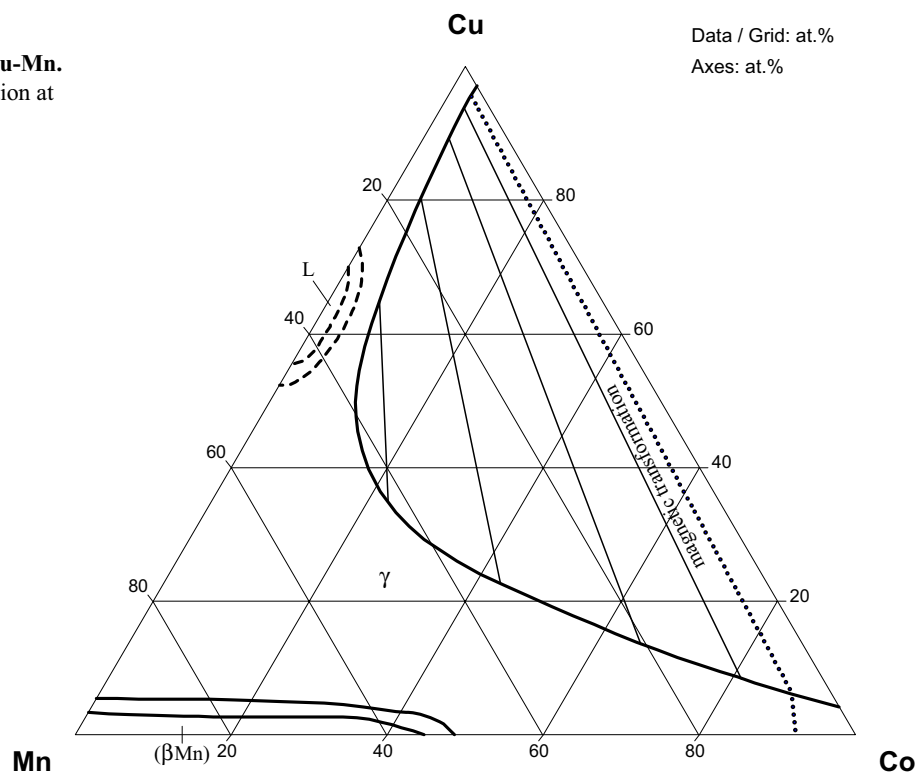


**Fig. 7: Co-Cu-Mn.**  
Isothermal section at  
777°C

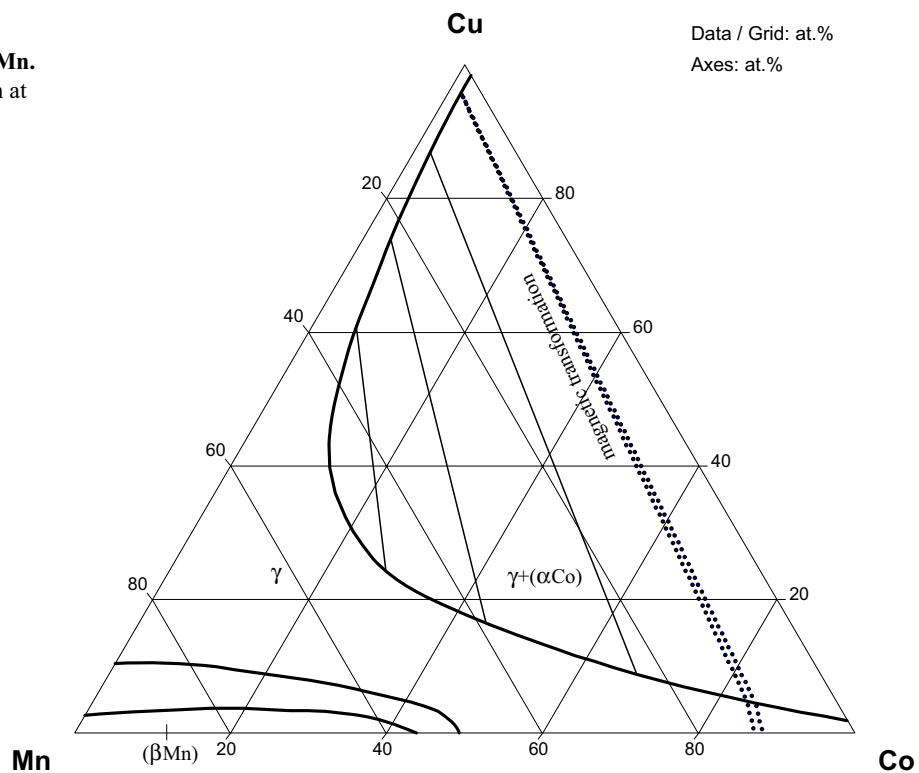




**Fig. 8: Co-Cu-Mn.**  
Isothermal section at  
577°C

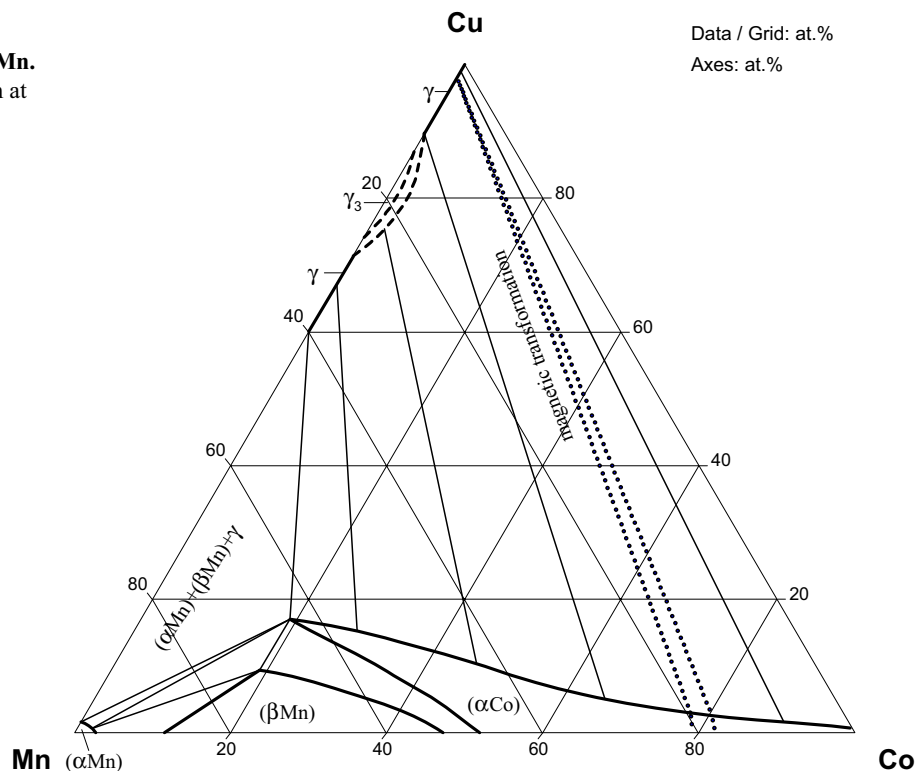


**Fig. 9: Co-Cu-Mn.**  
Vertical section at 10  
mass% Mn, plotted  
in at.%

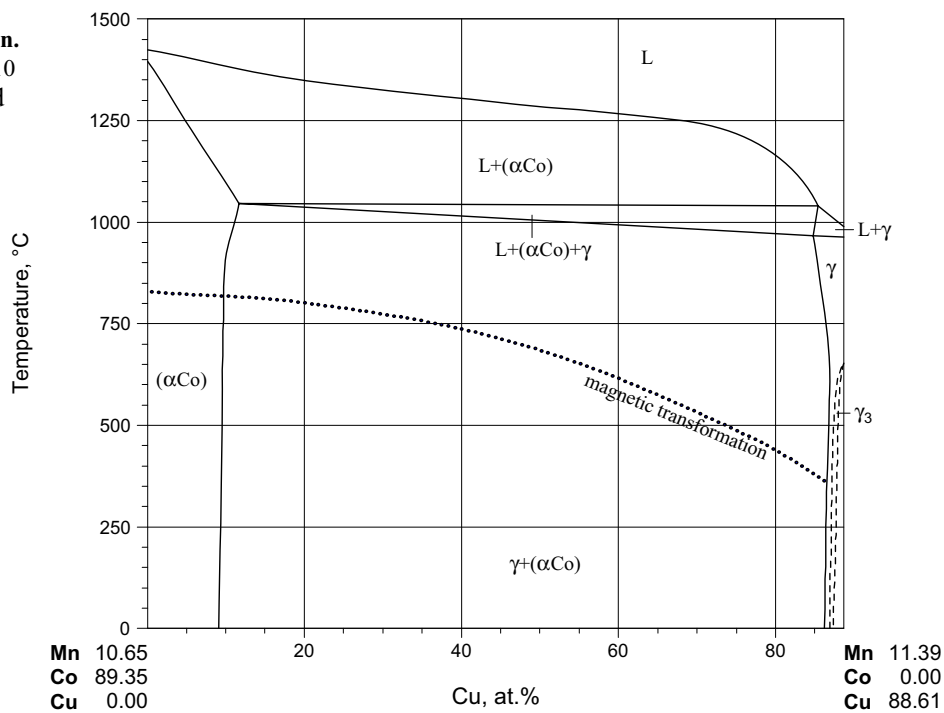


**Fig. 10: Co-Cu-Mn.**  
Vertical section at 30  
mass% Mn, plotted  
in at.%

